

IMAGING SPECTROMETER DATA ANALYSIS - A TUTORIAL

Fred A. Kruse
Center for the Study of Earth from Space (CSES)
Cooperative Institute for Research in Environmental Sciences (CIRES)
and
Department of Geological Sciences
University of Colorado, Boulder, CO 80309 USA

ABSTRACT

This tutorial is designed to provide an overview of selected methods for analysis of imaging spectrometer data. "Calibration" to reflectance is a prerequisite for most analysis approaches. A brief review of both empirical and model-based methods for recovery of apparent surface reflectance from the data is presented. Data analysis methods discussed include single pixel spectrum analysis, both empirical and feature based approaches to spectral classification of imaging spectrometer data, and the use of linear spectral unmixing to determine abundances of materials occurring with sub-pixel distributions.

1. INTRODUCTION

Visible/infrared optical remote sensing utilizes reflected solar energy to make measurements of the Earth's surface. Solar energy is scattered or absorbed based upon the physical properties and composition of the surface materials, and given sufficient spatial and spectral sensor resolution, these phenomena allow direct identification of individual materials. Multispectral remote sensing has been used routinely since the launch of Landsat in the early 1970s in disciplines as widely varying as geology, ecology, hydrology, oceanography, military applications, and many others. Imaging spectrometry or "hyperspectral" sensing has been available to government and university researchers for about 10 years, however, only recently have commercial and military end-users become aware of its potential.

1.1 WHAT IS IMAGING SPECTROMETRY (HYPERSPETRAL SENSING)

Broad-band remote sensing systems, such as the Landsat Multispectral Scanner (MSS, 4 bands) and Landsat Thematic Mapper (TM, 7 bands), drastically under sample the information content available from a reflectance spectrum by making only a few measurements in spectral bands up to several hundred nanometers wide. Imaging spectrometers, on the other hand, sample at close intervals (bands on the order of tens of nanometers wide) and have a sufficient number of spectral bands to allow construction of spectra that closely resemble those measured on laboratory instruments (Figure 1). Imaging spectrometry is defined as "the simultaneous acquisition of images in many narrow, contiguous spectral bands" (Goetz et al., 1985). Analysis of imaging spectrometer data allows extraction of a detailed spectrum for each picture element (pixel) of the image. High spectral resolution reflectance spectra collected by imaging spectrometers allow direct identification (and in some instances, abundance determinations) of individual materials based upon their reflectance characteristics including minerals (Goetz et al., 1985; Lang et al. 1987; Pieters and Mustard, 1988; Kruse, 1988; Kruse et al., 1993; Crowley, 1993; Boardman and Kruse, 1994), atmospheric constituent gases (Gao and Goetz, 1990; Carrère and Conel, 1993), vegetation (Gamon et al., 1993; Roberts et al., 1993; Elvidge et al., 1993), snow and ice (Nolin and Dozier, 1993), and dissolved and suspended constituents in lakes and other water bodies (Hamilton et al., 1993; Cardner et al., 1993).

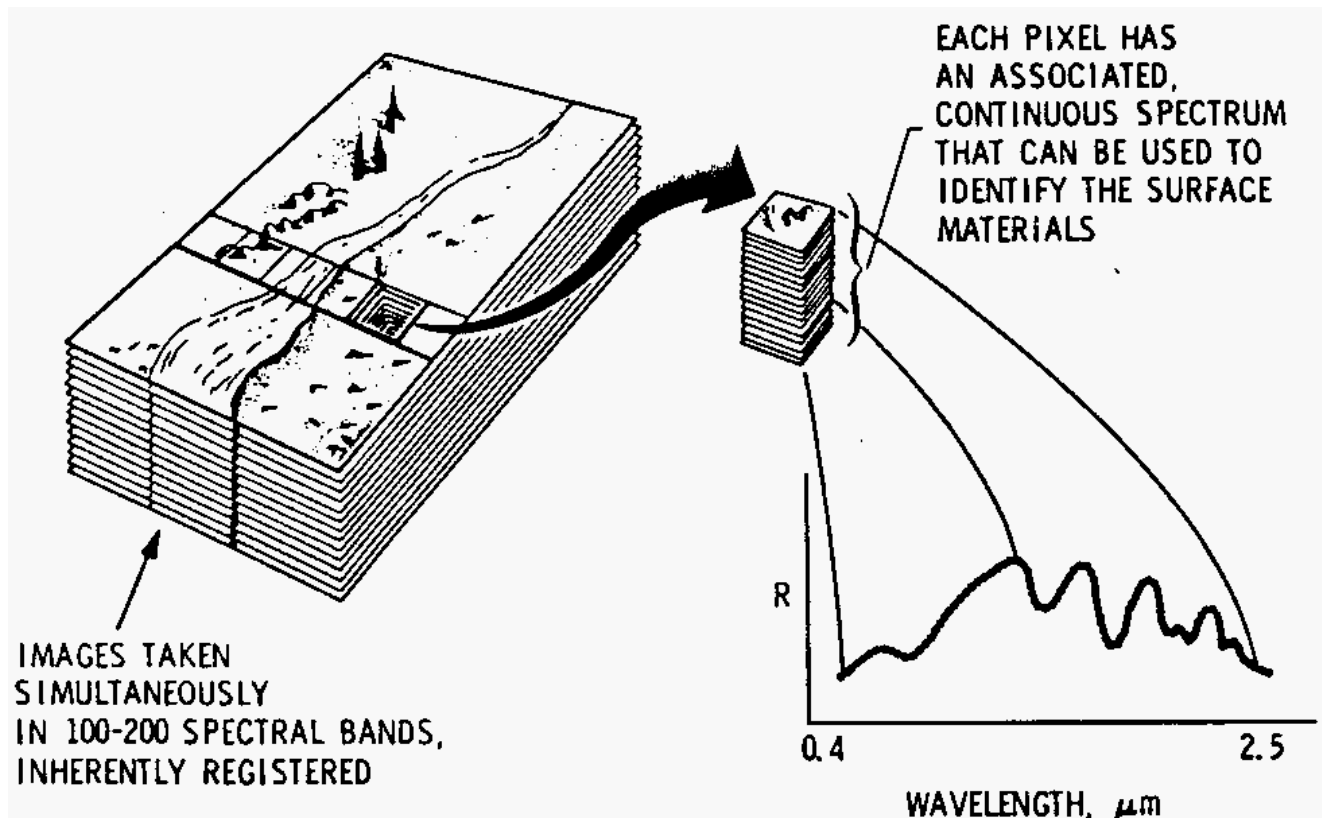


Figure 1. Schematic illustration of the imaging spectrometry concept. Images are acquired simultaneously of up to several hundred narrow spectral bands providing a complete reflectance spectrum for every pixel in the imaging spectrometer scene (from Vane, 1985).

1.2 REAL WORLD PROBLEMS

Theoretically, identification and mapping of individual materials using imaging spectroscopy should be quite easy. There are, however, significant factors that complicate the procedure. Remote sensing measurements of the Earth's surface are strongly influenced by the atmosphere (Goetz et al., 1985). Both scattering and absorption by gases and particulates affect the amount and wavelengths of light reaching the sensors. Absorption by atmospheric gases is dominated by water vapor with smaller contributions from carbon dioxide, ozone, and other gases (Gao and Goetz, 1990). Strong atmospheric water absorption bands make the atmosphere opaque in many regions (for example the 1.4 and 1.9 μm regions) and only small atmospheric windows are available for terrestrial remote sensing.

Additionally, visible/near-infrared remote sensing can provide compositional information only for approximately the top 50 μm of exposed surfaces (Buckingham and Sommer, 1983). Surface coatings or other differences between what is exposed at the surface versus what underlies the surface can mask near-surface spectral variation.

Determination of surface composition is also complicated by spectral mixing. Exposed surfaces are rarely composed of a single pure material. Intimate mixtures of varied materials are more common for naturally occurring materials such as rock and soils (Mustard and Pieters, 1987;

Boardman, 1989) and surfaces covered by vegetation are influenced by such factors as canopy architecture, shading, and vegetation density (Milton et al., 1983; Collins et al., 1983; Peterson et al., 1988; Roberts et al., 1993). Additionally, within typical instrument fields of view (10-100 m) materials are spatially mixed and the signal reaching the sensor is an areal average of the individual component signatures (Boardman, 1989, 1991; Boardman and Kruse, 1993).

2. CALIBRATION TO REFLECTANCE IS A PREREQUISITE TO MOST ANALYSIS

The most critical step in most imaging spectrometer data analysis strategies is to convert the data to reflectance so that individual spectra can be compared directly with laboratory or field data for identification. This requires that accurate wavelength calibration be performed. Laboratory measurements made before and after data acquisition usually provide the initial wavelength calibration. An additional check on the wavelength calibration can be made by comparing the positions of known atmospheric absorption features to their locations in the imaging spectrometer data. Atmospheric carbon dioxide (CO₂) absorption bands located at 2.005, and 2.055 μm are useful for wavelength-calibration of the data in the infrared (Kneisyz et al., 1988; Vane, 1987). In the visible and photographic infrared portion of the spectrum, narrow atmospheric water bands at 0.69, 0.72, and 0.76 μm can be used to calibrate wavelengths.

Ideally, imaging spectrometer data should be calibrated to absolute reflectance using onboard calibration. Onboard calibration, however, is typically not available. In its absence, several approaches have been used to calibrate the data to reflectance relative to a reference spectrum, "relative reflectance".

Marsh and McKeon (1983) used a multiplier to scale GERS Mark I spectra (a single pixel column of spectra, not true imaging spectrometer data) to a constant value at 2.04 μm . They then subtracted the average normalized radiance value for each channel from each normalized spectrum to produce a "residual image". For these line data, the residual image consisted of a number of color-coded, stacked spectra that enhanced regions with varying spectral characteristics.

A similar procedure ("logarithmic residuals", Green and Craig, 1985) has been used by numerous investigators to successfully map mineral distributions with imaging spectrometer data. The mathematically similar "internal average relative reflectance" (IAR reflectance) calibration has also been used with considerable success in arid regions (Kruse, 1988; Ben-Dor et al., 1994). IAR reflectance is calculated by determining an average spectrum for an entire imaging spectrometer data set and dividing each spectrum in the data set by the average spectrum. The resulting spectra represent reflectance relative to the average spectrum and resemble laboratory spectra acquired of the same materials (Kruse, 1988).

While all of these methods produce calibrated images and spectra with characteristics similar to reflectance, it is crucial to remember that these techniques produce relative reflectance not absolute reflectance. Any data set reduced to reflectance by division by a reference spectrum (flat field, log residual, or IAR) may have artifacts introduced by the fact that the reference spectrum itself may have spectral characteristics related to specific absorption features. This can adversely affect the appearance of the reflectance spectra and limit their usefulness in comparisons with laboratory spectra. One advantage of the techniques described above is that the conversion to apparent reflectance does not require *a priori* knowledge of the site.

2.1 EMPIRICAL LINE CALIBRATION

An alternative to onboard calibration or reflectance conversions based on internal characteristics of the data is to use a standard area on the ground to calibrate the data to reflectance (Ballew, 1975; Roberts et al., 1985; Elvidge 1988; Kruse et al., 1990; 1993), however, this approach requires *a priori* knowledge of each site. The calibration to reflectance requires choosing two or more ground target regions with albedos that span a wide range and acquiring field or laboratory spectra to characterize them. The second step in the process involves picking multiple pixels in the airborne data set that are associated with each ground target. Then a linear regression is calculated for each band to determine the gains and offsets required to convert the DN to reflectance. Solving the system of linear equations provides estimates of the standard error for each parameter at each wavelength in addition to the gain and offset spectra for use in the calibration. Bands with large total errors should be considered for deletion from the data set and further analysis efforts. The gain spectrum of the remaining bands is essentially a solar irradiance curve. The offset value spectrum is usually a correction that increases in magnitude with wavelength, and is essentially a path radiance term.

The final step in the spectral calibration is to multiply the instrument DN values by the proper gain factor and to add the corresponding offset value. The result is the removal of atmospheric effects (both attenuation and scattering), viewing geometry effects, and residual instrument artifacts. While no such correction can be perfect, the empirical line calibration does allow conversion of the remotely sensed spectra into a form that can be readily compared with laboratory or field acquired spectra. This technique does require field or laboratory spectra of at least two regions in the area of interest. It also makes the assumption that all of the image pixels chosen to characterize each ground spectrum represent identical composition and reflectance response.

2.2 CALIBRATION USING AN ATMOSPHERIC MODEL

Ideally, researchers would like to be able to calibrate their data to absolute reflectance rather than relative reflectance without actually having to make ground measurements. One method that comes close to achieving this goal is a radiative transfer model-based technique "The Atmospheric Removal Program" (ATREM) developed by Gao and Goetz (1990) and Gao et al. (1993) using 224-channel Airborne Visible/Infrared Imaging Spectrometer (AVIRIS) data (Porter and Enmark, 1987). Several similar atmospheric model programs being developed and tested by other researchers (Teillet, 1989; Green, 1991, Carrère and Conel, 1993). The ATREM method involves using a three-channel ratioing method that utilizes the 0.94 and 1.1 μm water vapor bands to calculate water vapor on a pixel-by-pixel basis from the AVIRIS data. Apparent reflectance spectra are first obtained by dividing each AVIRIS spectrum by the solar irradiance curve above the atmosphere (Kneisyz et al., 1988). A number of theoretical water vapor transmittance spectra for the 0.94 and 1.1 μm water vapor bands are calculated for varying amounts of atmospheric water vapor using an approximate radiative transfer code called "Simulation of the Satellite Signal in the Solar Spectrum (5S)" (Tanre et al., 1986) and the Malkmus (1967) narrow band spectral model. The modeled spectra are run through the three-channel ratioing method to generate a lookup table of water vapor concentrations that can be used to convert the AVIRIS apparent reflectance measurements to total column water vapor. The output of this procedure is an image showing the spatial distribution of various water vapor concentrations as derived for each pixel of the AVIRIS data. The water vapor image is then used along with transmittance spectra derived for each of atmospheric gases CO_2 , O_3 , N_2O , CO , CH_4 , and O_2 using the Malkmus narrow band model and 5S model to produce scaled surface reflectance (Teillet, 1989, Gao and Goetz, 1990, Gao et al., 1993). This model-based technique produces total water vapor column images and reflectance calibrated AVIRIS data without *a priori* knowledge. This model has

also successfully been applied to Geophysical and Environmental Research (GER) 63-band scanner data (Personal communication, Eyal Ben-Dor).

3. SELECTED DATA ANALYSIS METHODS

A great deal of spectral information can be extracted from either raw or calibrated imaging spectrometer data using "standard" image processing procedures but new techniques are required to take full advantage of the data. Successful discrimination of varied lithologies has been demonstrated using simple procedures such as color compositing, band ratios, and principal components (Feldman and Tarani, 1988) and more advanced procedures such as Chebyshev waveform analysis (Collins et al., 1983). Empirically-based procedures like those mentioned above, however, usually represent underutilization of the data, although they may actually enhance the information available from noisy data sets. Display of imaging spectrometer data is more complex than displaying three bands as a RGB color composite. The information present in the imaging spectrometer data simply cannot be fully displayed in one, or even 10, color images. A combination of spectral and spatial domains must be used to fully display the compositional information present in the data.

3.1 SINGLE PIXEL SPECTRUM BROWSING

Several public domain and commercial software packages are available that allow users to make direct comparisons between image and reference spectra (Mazer et al. 1988; Torson et al. 1989, Kruse et al., 1993). The first step after calibrating any imaging spectrometer data set is to look at the data in both the spatial and spectral domains. Ideally, this is done simultaneously by selecting a location on a single band or color composite and extracting the individual spectrum or by outlining a region of interest and extracting the average spectrum. Visual comparison is usually used to assess the calibration quality and to compare the extracted spectra to a spectral library or reference spectrum.

3.2 EMPIRICAL-BASED APPROACHES TO SPECTRAL CLASSIFICATION

The simplest way to produce maps showing the spatial distribution of specific materials using imaging spectrometer data is to empirically match image spectra to reference spectra. The reference spectra can be either laboratory or field spectra or extracted from the imaging spectrometer data. The Spectral Angle Mapper" (SAM) is one algorithm designed to determine the similarity of spectra in multidimensional space (Boardman personal communication, 1991; Yuhas et al., 1993). This method assumes that the data have been reduced to apparent reflectance. The algorithm determines the similarity between two spectra by calculating the "angle" between them, treated as vectors in a space with dimensionality equal to the number of bands (nb).

A simplified explanation of this can be given by considering a reference spectrum and a test spectrum from 2-band data represented on a two-dimensional plot as two points. The lines connecting each spectrum-point and the origin contain all possible positions for that material, corresponding to the range of possible illuminations. Poorly illuminated pixels will fall closer to the origin (the dark point) than pixels with the same spectral signature but greater illumination. The angle between the vectors, however, is the same regardless of their length. The SAM algorithm generalizes this geometric interpretation to nb-dimensional space. The calculation consists of taking the arccosine of the dot product of the spectra. This measure of similarity is insensitive to gain factors because the angle between two vectors is invariant with respect to the lengths of the vectors. As a result, laboratory spectra can be directly compared to remotely sensed apparent reflectance spectra, which inherently have an unknown gain factor related to topographic illumination effects.

For each reference spectrum, the spectral angle is determined for every image spectrum and this value, in radians, is assigned to that pixel in an output SAM image for that reference material.

The derived spectral angle image maps form a new data cube with the number of bands equal to the number of reference spectra used in the mapping. The results for each reference spectrum are typically viewed separately as gray-scale images or combined to form a color composite. Small spectral angles correspond to high similarity and these pixels are usually shown in brighter gray levels. Larger angles, corresponding to less similar spectral shapes, are shown in darker gray levels.

3.3 ABSORPTION FEATURE-BASED CHARACTERIZATION AND MAPPING

Many researchers have concentrated on the use of specific absorption features in reflectance spectra to identify specific materials (Green and Craig, 1985; Kruse et al., 1985; Yamaguchi and Lyon, 1986; Clark et al., 1987). Only recently have attempts been made to apply these techniques to imaging spectrometer data (Kruse, 1988; Clark et al., 1991; Abrams and Hook, 1990). The approach described here, an expert system, has been moderately successful in identifying mineralogy in arid terrains using AVIRIS data.

An expert system approach developed at CSES allows automated identification of Earth surface materials based on their spectral characteristics in imaging spectrometer data (Kruse et al., 1993). This expert system requires that the imaging spectrometer data be calibrated to reflectance because rules for identification are built using laboratory reflectance spectra. Once the data are properly calibrated, the procedure is to treat each pixel individually and sequentially to remove a continuum (normalize), binary encode the spectrum (Mazer et al., 1988), extract the features, and compare the binary encoding and features to the binary encoded reference spectrum and the feature rules built from the spectral library of reference materials. The result of these analyses is a new data cube consisting of a single image for each endmember contained in the spectral library (Kruse and Lefkoff, 1993). These images contain a value for each pixel indicating an empirical probability that a particular material will occur at that location. Probabilities range from 0.0 to 1.0 with 1.0 indicating a perfect match.

More specifically, the procedure is as follows. A spectral library of laboratory reference spectral reflectance measurements is used to develop a generalized knowledge base for analysis of visible and infrared reflectance spectra. Several libraries are available in the public domain (Clark et al., 1990; Grove et al., 1992). Spectral features are digitally extracted from a spectral library and numerical analysis and characterization of the digital reflectance measurements are used to establish quantitative criteria for identifying materials.

Absorption feature information is extracted from laboratory spectra (and later each image spectrum) using the following automated techniques (Kruse et al., 1988; 1993).

- 1). A continuum is defined for each spectrum by finding the high points (local maxima) and fitting straight line segments between these points.
- 2). The continuum is divided into the original spectrum to normalize the absorption bands to a common reference. (See Clark and Roush, 1984 for a discussion of division versus subtraction of the continuum).
- 3). The minima of the continuum-removed spectrum are determined and the 10 strongest absorption features extracted.
- 4). The wavelength position, depth, full width at half the maximum depth (FWHM), and asymmetry for each of these 10 features are determined and tabulated. The asymmetry

is defined as the sum of the reflectance values for feature channels to the right of the minimum divided by the sum of the reflectance values for feature channels to the left of the minimum. The base ten logarithm is taken of this value to maintain linearity. Symmetrical bands thus have an asymmetry value of zero (the area to the left and right of the band center are equal). Bands that are asymmetrical towards shorter wavelengths have negative asymmetry, while bands that are asymmetrical towards longer wavelengths have positive asymmetry. The magnitude of the asymmetry value indicates the degree of asymmetry.

The information derived from the analysis of the spectral library are interactively reviewed simultaneously in both tabular and graphical format to determine if features extracted from the digital spectra are representative of the material measured or were due to impurities. The four parameters derived using the feature extraction procedure are used in conjunction with published spectral information to determine the critical absorption bands and absorption band characteristics for identification of specific materials. Facts and rules are formulated based on the analysis of the reference spectra.

The final step is to apply the rules to an imaging spectrometer data set to automatically identify materials and to map their spatial distributions. The absorption feature positions and shapes of each reflectance spectrum for each picture element (pixel) are characterized using the automated techniques described previously for individual laboratory spectra. The final products of the expert system analysis are a "continuum-removed" cube with "n" bands containing all of the continuum-removed spectra calculated from the reflectance data, a "feature" cube containing the wavelength positions, depths, FWHMs, and asymmetries for each pixel for the ten strongest absorption features, and an "analysis cube" showing the location and probability of occurrence of the reference materials based on a weighted combination of binary encoding, and feature analysis in the expert system. The analysis cube also contains four images that help with evaluation of the expert system mapping success. These are 1) the "final decision best endmember" image showing the single best match for each pixel, 2) the "sum of decisions" image showing the sum of all probabilities for each pixel, 3) the "number of decisions greater than or equal to 50%" image showing those areas with endmembers with high probabilities, and 4) the "no match" image showing those areas with maximum probabilities less than or equal to 10%.

Interactive display and analyses of the probability images and the additional images described above permits determination of the spatial extent of specific minerals and identification of problem areas where the expert system may have identified multiple minerals, or no minerals at all. These images form the starting point for detailed analyses using techniques such as linear spectral unmixing.

3.4 SPECTRAL UNMIXING

Identification of the main constituents of the surface is only the first step in mapping using imaging spectrometer data because natural surfaces are rarely composed of a single uniform material. These surfaces are more commonly made up of mixtures or assemblages of intimately mixed minerals, alteration products, or weathered constituents; and vegetation, water, and shadows. Spectral mixing is a consequence of the mixing of materials having different spectral properties within the ground field-of-view (GFOV) of a single image pixel. Several researchers have investigated mixing scales and linearity. Singer and McCord (1979) found that if the scale of the mixing is large (macroscopic), then the mixing occurs in a linear fashion. For microscopic or intimate mixtures, the mixing is generally nonlinear (Nash and Conel, 1974; Singer, 1981).

Boardman (1989, 1991) addressed the macroscopic mixing problem using singular value matrix decomposition (SVD) to determine the scale of spatial mixing and to linearly unmix AVIRIS data. This technique assumes that most mixing is on the macroscopic scale, and thus linear. For most situations, however, there is a significant amount of intimate mixing and therefore the linear unmixing techniques are at best an approximation. Abundances determined using these techniques are not as accurate as those determined using non-linear techniques, however, to the first order, they appear to adequately represent the surface conditions.

A spectral library of constituent spectra or "endmembers" typically forms the initial data matrix for the analysis. Ideally, these endmembers, when linearly combined should be able to match all possible spectra in the imaging spectrometer data. An inverse of the spectral library matrix is formed by multiplying together the transposes of the orthogonal matrices and the reciprocal values of the diagonal matrix (Boardman, 1989). A simple vector-matrix multiplication between the inverse library matrix and an observed mixed image spectrum gives an estimate of the abundance of the library endmembers for the unknown spectrum.

Data are typically first examined using unconstrained unmixing in which the derived abundances are free to take on any value including negative ones. The output of the unmixing process is an image data cube with the same spatial dimensions as the input data, with the "spectral" output bands representing the abundances of the endmembers. The analysis also usually produces two additional images, one showing the sum of the abundances at each pixel, and the other the root-mean-square (rms) error values at each pixel. Interactive analysis of the abundance cube, the sum image, and the rms error image is used to determine if the endmembers explain most of the spectral variation. Subsequent inclusion of new endmembers and iteration are used until the rms error is small and the results converge to non-negative values that sum to one or less (100%). Alternatively, fully constrained unmixing may be used, but this is much more computationally intensive.

4. CONCLUSIONS

This paper presents an overview of several commonly used imaging spectrometer data analysis techniques. There are as many different approaches, however, to working with these data as there are spectral bands in a typical data set. A complete analysis usually combines the use of spatial and spectral processing, analysis, and interpretation. The reader is referred to the current literature for detailed discussion of the many options.

REFERENCES

- Ballew, G., 1975, A method for converting Landsat I MSS data to reflectance by means of ground calibration sites: Stanford Remote Sensing Laboratory Technical Report 75-5, Stanford, CA.
- Ben-Dor, E., and Kruse, F. A., 1994, The relationship between the size of spatial subsets of GER 63 channel scanner data and the quality of the Internal Average Relative Reflectance (IARR) correction technique: International Journal of Remote Sensing, v. 15, no. 3, p. 683-690.
- Boardman, J. W., 1989, Inversion of imaging spectrometry data using singular value decomposition: in Proceedings, IGARSS '89, 12th Canadian Symposium on Remote Sensing, 4, pp. 2069-2072.
- Boardman, J. W. , 1991, Sedimentary Facies Analysis Using Imaging Spectrometry: A Geophysical Inverse problem: Unpublished Ph. D. Thesis, University of Colorado, Boulder, 212 p.

- Boardman, J. W., and Kruse, F. A., 1994, Automated spectral analysis: A geological example using AVIRIS data, northern Grapevine Mountains, Nevada: in Proceedings, Tenth Thematic Conference, Geologic Remote Sensing, 9-12 May 1994, San Antonio, Texas, p. I-407 - I-418.
- Buckingham, W. F., and Sommer, S. E., 1983, Mineralogical characterization of rock surfaces formed by hydrothermal alteration and weathering-Application to remote sensing: Economic Geology, v. 78, no. 4, p. 664-674.
- Carder, K. L., Reinersman, P., Chen, R. F., Muller-Karger, F., Davis, C. O., and Hamilton M. K., 1993: AVIRIS calibration and application in coastal oceanic environments: Remote Sensing of Environment, v. 44, nos. 2-3, p. 205 - 216.
- Carrère, V., and Conel, J., 1993, Recovery of atmospheric water vapor total column abundance from imaging spectrometer data around 940 nm - Sensitivity analysis and application to Airborne Visible/Infrared Imaging Spectrometer (AVIRIS) data: Remote Sensing of Environment, v. 44, nos. 2-3, p. 179 - 204.
- Clark, R. N., and Roush, T. L., 1984, Reflectance spectroscopy: Quantitative analysis techniques for remote sensing applications: Journal of Geophysical Research, v. 89, no. B7, pp. 6329-6340.
- Clark, R. N., King, T. V. V., Klejwa, M., and Swayze, G. A., 1990, High spectral resolution spectroscopy of minerals: Journal of Geophysical Research, v. 95, no. B8, p. 12653-12680.
- Clark, R. N., King, T. V. V., and Gorelick, N. S., 1987, Automatic continuum analysis of reflectance spectra: in Proceedings, Third AIS workshop, 2-4 June, 1987, JPL Publication 87-30, Jet Propulsion Laboratory, Pasadena, California, p. 138-142.
- Clark, R. N., Swayze, G. A., Gallagher, A., Gorelick, N., and Kruse, F. A., 1991, Mapping with imaging spectrometer data using the complete band shape least-squares algorithm simultaneously fit to multiple spectral features from multiple materials: in Proceedings, 3rd Airborne Visible/Infrared Imaging Spectrometer (AVIRIS) workshop, JPL Publication 91-28, p. 2-3.
- Collins, W. et al., 1983, Airborne biogeochemical mapping of hidden mineral deposits: Economic Geology, v. 78, p. 737-749.
- Crowley, J. K., 1993 Mapping playa evaporite mineral with AVIRIS data: A first report from Death Valley, California: Remote Sensing of Environment, v. 44, nos. 2-3, p. 337 - 356.
- Elvidge, C. D., 1988, Vegetation reflectance features in AVIRIS data: in Proceedings, International Symposium on Remote Sensing of Environment, Sixth Thematic Conference, "Remote Sensing for Exploration Geology", Houston, Tx, 16--19 May, 1988, Environmental Research Institute of Michigan, Ann Arbor, p. 169-182.
- Elvidge, C. D., Chen, Z., and Groeneveld, D. P., 1993, Detection of trace quantities of green vegetation in 1990 AVIRIS data: Remote Sensing of Environment, v. 44, nos. 2-3, p. 271 - 280.
- Feldman, S., and Taranik, J. V., 1988, Comparison of techniques for discriminating hydrothermal

alteration minerals with Airborne Imaging spectrometer data: Remote Sensing of Environment, 24, 1, 67-83.

- Gamon, J. A., Field, C. B., Roberts, D. A., Ustin, S. L., and Valentini, R., 1993, Functional patterns in an annual grassland during and AVIRIS overflight: Remote Sensing of Environment, v. 44, nos. 2-3, p. 239 - 254.
- Gao B. and Goetz, A. F. H., 1990, Column atmospheric water vapor and vegetation liquid water retrievals from airborne imaging spectrometer data: Journal of Geophysical Research, v. 95, no. D4, p. 3549-3564.
- Gao, B., Heidebrecht, K. B., and Goetz, A. G. H., 1993, Derivation of scaled surface reflectances from AVIRIS data: Remote Sensing of Environment, v. 44, nos. 2-3, p. 165-178.
- Goetz, A. F. H., Vane, G., Solomon, J. E., and Rock, B. N., 1985, Imaging spectrometry for earth remote sensing: Science, 228, 1147-1153.
- Green, A. A., and Craig, M. D., 1985, Analysis of aircraft spectrometer data with logarithmic residuals: in Proceedings, AIS workshop, 8-10 April, 1985, JPL Publication 85-41, Jet Propulsion Laboratory, Pasadena, California, p. 111-119.
- Green, R. O., 1991, Retrieval of reflectance from AVIRIS-measured radiance using a radiative transfer code: in Proceedings, 3rd Airborne Visible/Infrared Imaging Spectrometer (AVIRIS) workshop, JPL Publication 91-28, p. 200-210.
- Grove, C. I., Hook, S. J., and Paylor, E. D., Laboratory reflectance spectra of 160 minerals, 0.4 to 2.5 micrometers: JPL Publication 92-2.
- Hamilton, M. K., Davis, C. O., Rhea, W. J., Pilorz, S. H., and Carder, K. L., 1993, Estimating chlorophyll content and bathymetry of Lake Tahoe using AVIRIS data: Remote Sensing of Environment, v. 44, nos. 2-3, p. 217 - 230.
- Hook, S. J., and Rast, M., 1990, Mineralogic mapping using Airborne Visible/Infrared Imaging Spectrometer (AVIRIS) shortwave infrared (SWIR) data acquired over Cuprite, Nevada: in Proceedings, 2nd Airborne Visible/Infrared Imaging Spectrometer (AVIRIS) workshop, JPL Publication 90-54, p. 199-207.
- Kneisyz, F. X., Shettle, E. P., Abreau, L. W., Chetwynd, J. H., Anderson, G. P., Gallery, W. O., Selby, E. A., and Clough, S. A., 1988, Users guide to LOWTRAN 7, AFGL-TR-8-0177, Airforce Geophysics Laboratory, Bedford, MA.
- Kruse, F. A., Raines, G. L., and Watson, Kenneth, 1985, Analytical techniques for extracting geologic information from multichannel airborne spectroradiometer and airborne imaging spectrometer data: in Proceedings, International Symposium on Remote Sensing of Environment, Fourth Thematic Conference, "Remote Sensing for Exploration Geology", San Francisco, California, 1-4 April, 1985, p. 309-324.
- Kruse, F. A., 1988, Use of Airborne Imaging Spectrometer data to map minerals associated with hydrothermally altered rocks in the northern Grapevine Mountains, Nevada and California:

Remote Sensing of Environment, v. 24, no. 1, pp. 31-51.

- Kruse, F. A., Kierein-Young, K. S., and Boardman, J. W., 1990, Mineral mapping at Cuprite, Nevada with a 63 channel imaging spectrometer: Photogrammetric Engineering and Remote Sensing, v. 56, no. 1, pp. 83-92.
- Kruse, F. A., Lefkoff, A. B., Boardman, J. B., Heidebrecht, K. B., Shapiro, A. T., Barloon, P. J., and Goetz, A. F. H., 1993, The Spectral Image Processing System (SIPS) - Interactive Visualization and Analysis of Imaging Spectrometer Data: Remote Sensing of Environment, Special issue on AVIRIS, May-June 1993, v. 44, p. 145 - 163.
- Kruse, F. A., Lefkoff, A. B., and Dietz, J. B., 1993, Expert System-Based Mineral Mapping in northern Death Valley, California/Nevada using the Airborne Visible/Infrared Imaging Spectrometer (AVIRIS): Remote Sensing of Environment, Special issue on AVIRIS, May-June 1993, v. 44, p. 309 - 336.
- Kruse, F. A., and Lefkoff, A. B., 1993, Knowledge-based geologic mapping with imaging spectrometers: Remote Sensing Reviews, Special Issue on NASA Innovative Research Program (IRP) results, v. 8, p. 3 - 28.
- Lang, H. R., Adams, S. L., Conel, J. E., McGuffie, B. A., Paylor, E. D., and Walker, R. E., 1987, Multispectral remote sensing as stratigraphic tool, Wind River Basin and Big Horn Basin areas, Wyoming: American Association of Petroleum Geologists Bulletin, 71, 4, 389-402.
- Nash, E. B., and Conel, J. E. (1974) Spectral reflectance systematics for mixtures of powdered hypersthene, labradorite, and ilmenite, Journal of Geophysical Research, 79, 1615-1621.
- Nolin, a. W., and Dozier, J., 1993, Estimating snow grain size using AVIRIS data: Remote Sensing of Environment, v. 44, nos. 2-3, p. 231 - 238.
- Malkmus, W., 1967, Random Lorentz band model with exponential-tailed S line intensity distribution function: J. Opt. Soc. Am., v 57, p. 323-329.
- Marsh, S. E., and McKeon, J. B., 1983, Integrated analysis of high-resolution field and airborne spectroradiometer data for alteration mapping: Economic Geology, v. 78, no. 4, p. 618-632.
- Mazer, A. S., Martin, M., Lee, M., and Solomon, J. E., 1988, Image processing software for imaging spectrometry data analysis: Remote Sensing of Environment, v. 24, no. 1, pp. 201-210.
- Milton, N. M., Collins, W., Chang, S. H., and Schmidt, R. G., 1983, Remote detection of metal anomalies on Pilot Mountain, N. Carolina: Economic Geology, v. 78, p. 605-617.
- Mustard, J. F., and Pieters, C. M., 1987, Abundance and distribution of ultramafic microbreccia in Moses Rock dike: Quantitative application of mapping spectroscopy: Journal of Geophysical Research, 92, B10, 10376-10390.
- Peterson, D. L., Aber, J. D., Matson, P. A., Card, D. H., Swanberg, N., Wessman, C., and Spanner, M., 1988, Remote sensing of forest canopy and leaf biochemical contents: Remote Sensing of Environment, v. 24, no. 1, pp. 85 - 108.

- Porter, W. M., and Enmark, H. T., 1987 A system overview of the Airborne Visible/Infrared Imaging Spectrometer (AVIRIS): in Proceedings, 31st Annual International Technical Symposium, Society of Photo-Optical Instrumentation Engineers, v. 834, pp. 22-31.
- Roberts, D. A., Yamaguchi, Y., and Lyon, R. J. P. (1985), Calibration of Airborne Imaging Spectrometer Data to percent reflectance using field spectral measurements: in Proceedings, Nineteenth International Symposium on Remote Sensing of Environment, Ann Arbor, Michigan, October 21-25, 1985.
- Singer, R. B., 1981, Near-infrared spectral reflectance of mineral mixtures: Systematic combinations of pyroxenes, olivine, and iron oxides: Journal of Geophysical Research, 86, 7967-7982.
- Singer, R. B., and McCord, T. B., 1979, Mars: Large scale mixing of bright and dark surface materials and implications for analysis of spectral reflectance: in Proceedings Lunar and Planetary Science Conference, 10th, p. 1835-1848.
- Tanre, D., Deroo, C., Duhaut, P., Herman, M., Morchrette, J. J., Perbos, J., and Deschamps, P. Y., 1986, Simulation of the Satellite Signal in the Solar Spectrum (5S), Users's Guide (U. S. T. de Lille, 59655 Villeneuve d'ascq, France: Laboratoire d'Optique Atmospherique).
- Teillet, P. M., 1989, Surface reflectance retrieval using atmospheric correction algorithms: in Proceedings of IGARSS'89 and the 12th Canadian Symposium on Remote Sensing, Vancouver, Canada, p. 864-867.
- Torson, J. M. (1989), Interactive image cube visualization and analysis: in Proceedings, Chapel Hill Workshop on Volume Visualization, 18-19 May, 1989, University of North Carolina at Chapel Hill.
- Vane, Gregg, 1987, First results from the Airborne Visible/Infrared Imaging Spectrometer (AVIRIS): in Proceedings, 31st Annual International Technical Symposium, Society of Photo-Optical Instrumentation Engineers, v. 834, p. 166-174.
- Vane, G., 1985, High spectral resolution remote sensing of the earth, Sensors, V.2, p. 11-20.
- Yamaguchi, Yasushi, and Lyon, R. J. P., 1986, Identification of clay minerals by feature coding of near-infrared spectra: in Proceedings, International Symposium on Remote Sensing of Environment, Fifth Thematic Conference, "Remote Sensing for Exploration Geology", Reno, Nevada, 29 September- 2 October, 1986, Environmental Research Institute of Michigan, Ann Arbor, p. 627-636.
- Yuhas, R. H. and Goetz, A. F. H., 1993, Comparison of airborne (AVIRIS) and Spaceborne (TM) imagery data for discriminating among semi-arid landscape endmembers: in Proceedings, Ninth Thematic Conference on Geologic Remote Sensing, Environmental Research Institute of Michigan, Ann Arbor, MI., p. 503 - 511.